

## Magnetic phase diagram of $\text{FeCl}_2 \cdot 2\text{H}_2\text{O}$

H. Weitzel and J. Hirte

*Institut für Physikalische Chemie, Fachgebiet Strukturforschung, Technische Hochschule,  
D-6100 Darmstadt, Federal Republic of Germany*

(Received 18 May 1987; revised manuscript received 26 October 1987)

$\text{FeCl}_2 \cdot 2\text{H}_2\text{O}$  represents a metamagnet, which shows two jumps in the magnetization at temperatures below a critical endpoint (4.3 T; 11.2 K), if a magnetic field is applied along the easy direction  $\alpha$ . Below 11.2 K, with increasing field, an antiferromagnetic zero-field phase is followed by a ferrimagnetic and the paramagnetic saturated phase. By means of neutron diffraction in fields up to 6.4 T and magnetization experiments up to 15 T, magnetic phase diagrams were determined for applied fields out of the easy direction  $\alpha$  as well for the intermediate direction  $\beta$  and the hard direction  $\gamma$  as for the total  $\alpha$ - $\beta$  plane. In particular, it should be emphasized that the ferrimagnetic phase does not disappear in this  $\alpha$ - $\beta$  plane going from the direction  $\alpha$  to the direction  $\beta$ . Furthermore, an increasing Néel temperature has been observed for fields along the direction  $\beta$ . Calculations of the  $H_\alpha$ - $H_\beta$  phase diagram at 0 K do not agree with the experiments, if well-known formulas for the exchange constants and the single-ion anisotropy are taken into account. If a simple assumption about the field dependence of one exchange constant is made, the agreement is excellent.

### I. INTRODUCTION

Numerous papers have been published about the magnetic properties of the metamagnet  $\text{FeCl}_2 \cdot 2\text{H}_2\text{O}$  (FC2) during the last two decades. These began with susceptibility and magnetization experiments<sup>1</sup> as well as the determination of the magnetic structures.<sup>2</sup> Below the Néel temperature,  $T_N = 21.5$  K, in increasing magnetic fields, a uniaxial, antiferromagnetic structure (the AF phase) is followed by a uniaxial, ferrimagnetic phase (the FI phase).<sup>2</sup> The magnetic field  $H_\alpha$  must be applied along the easy direction  $\alpha$  of the magnetization, and the temperature must be below 11.2 K in order to observe the FI phase. The transition field from the AF to the FI phase is denoted as  $H_\alpha^{\text{AF-FI}}$ . Furthermore, there exists a second transition field  $H_\alpha^{\text{FI-P}}$  from the FI phase to the paramagnetic saturated phase (the P phase).<sup>2</sup> FC2 crystallizes in the space group  $C2/m$  with Fe ions at the origin of the chemical unit cell and in the center of the  $a$ - $b$  plane. Figure 1(a) shows the magnetic structure of the AF and the FI phases. In both, the easy direction  $\alpha$  forms an angle of  $32.9^\circ$  with the  $c$  axis of the crystal lying within the  $a$ - $c$  quadrant. The  $\beta$  axis of the susceptibility tensor, which is perpendicular to the direction  $\alpha$ , lies likewise within the  $a$ - $c$  plane. Based on susceptibility measurements, the  $\beta$  axis is equivalent to the  $\gamma$  axis, which is parallel to the  $b$  axis of the crystal.<sup>1</sup> The magnetic  $H_\alpha$ - $T$  phase diagram was determined by experiments.<sup>3</sup> This included the critical behavior along the AF-P phase boundary at which, as a peculiarity, an AF-, FI-, and P-coexistence point at 4.3 T and 11.2 K was found as a critical endpoint.<sup>4</sup> Lastly, the magnetism of FC2 was examined theoretically.<sup>5,6</sup>

In FC2, the magnetic moments are coupled along the  $c$  axis by a ferromagnetic intra-chain-exchange constant,  $J_0 = 1.9 \text{ cm}^{-1}$ , forming ferromagnetic chains along this axis. These chains are coupled together by three inter-chain-exchange interactions. The first constant,

$J_1 = -0.27 \text{ cm}^{-1}$ , reaches from the cell origin to the center of the  $a$ - $b$  basis plane and couples together the chains antiferromagnetically. This results in an antiferromagnetic structure with a unit cell identical to the chemical one. Second, there exists a weak exchange constant,  $J_2 = -0.044 \text{ cm}^{-1}$ , along the  $a$  axis, and third a very weak exchange constant,  $J_3 < 0.01 \text{ cm}^{-1}$ , along the  $b$  axis. The last one is neglected in the following because it is very weak as a consequence of the two water molecules lying directly on the connecting line between the Fe ions. Nevertheless, this third interaction exists and must be

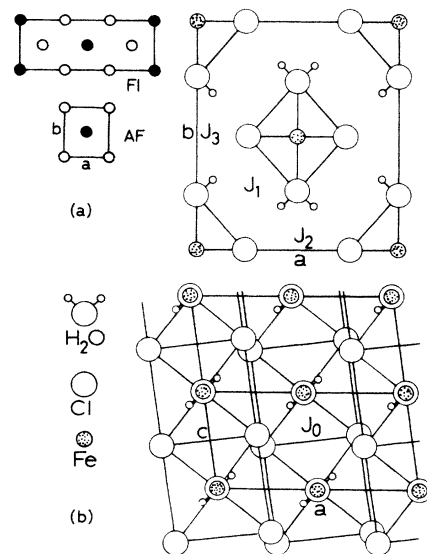


FIG. 1. (a) Antiferromagnetic and ferrimagnetic structures of  $\text{FeCl}_2 \cdot 2\text{H}_2\text{O}$ . (b) Projection of the crystal structure of  $\text{FeCl}_2 \cdot 2\text{H}_2\text{O}$  upon the  $a$ - $b$  plane and the  $a$ - $c$  plane (two unit cells), respectively.

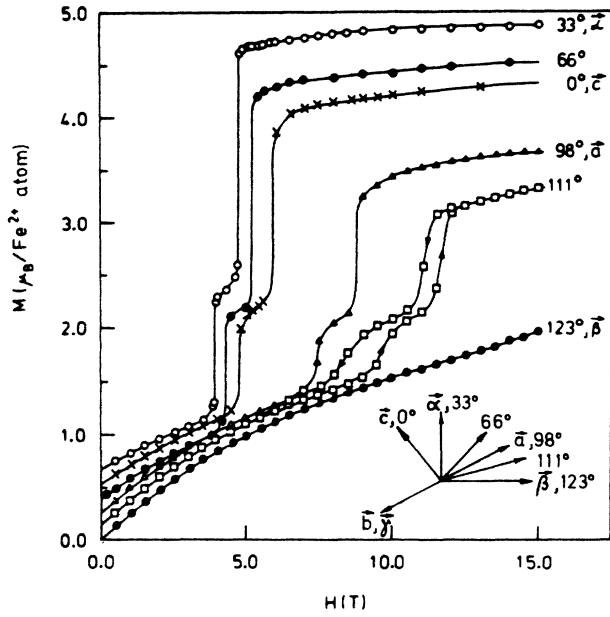


FIG. 2. Magnetization measurements of  $\text{FeCl}_2 \cdot 2\text{H}_2\text{O}$  at 4.2 K for different field directions within the  $a$ - $c$  plane.

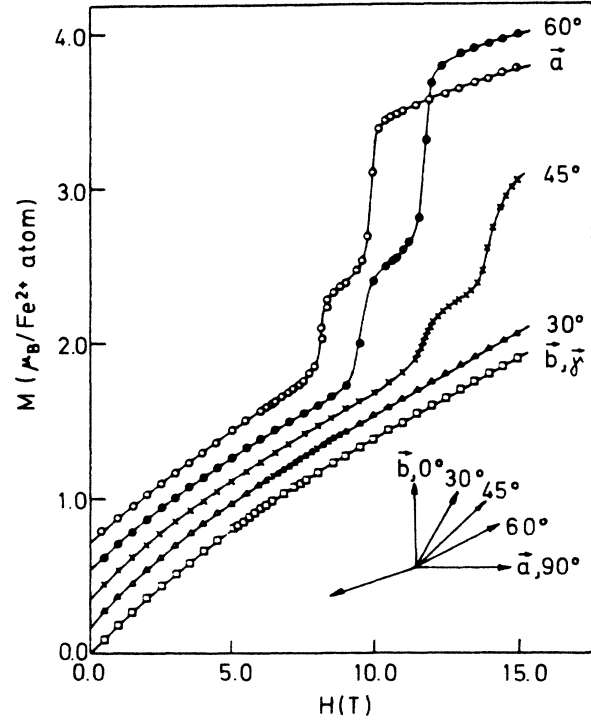


FIG. 4. Magnetization measurements of  $\text{FeCl}_2 \cdot 2\text{H}_2\text{O}$  at 4.2 K for different field directions within the  $a$ - $b$  plane.

positive in order to stabilize the observed FI phase with a tripled  $a$  axis and a magnetization  $\frac{1}{3}$  of the saturation value, against all other unobserved kinds of FI phases; for instance, phases with a magnetization  $\frac{1}{2}$  that of the saturated phase.<sup>7</sup> Figure 1(b) shows the crystal structure of FC2 from two different projections and the geometry of the exchange-interaction paths. The anisotropy in FC2 is included in the Hamiltonian by an additional single-ion

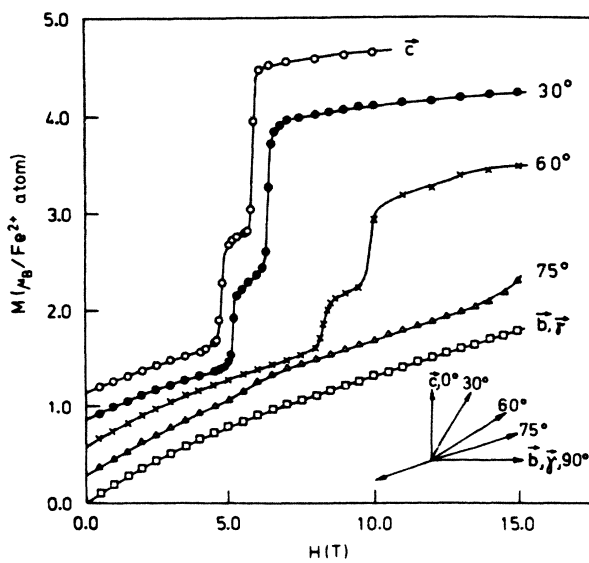


FIG. 3. Magnetization measurements of  $\text{FeCl}_2 \cdot 2\text{H}_2\text{O}$  at 4.2 K for different field directions within the  $b$ - $c$  plane.

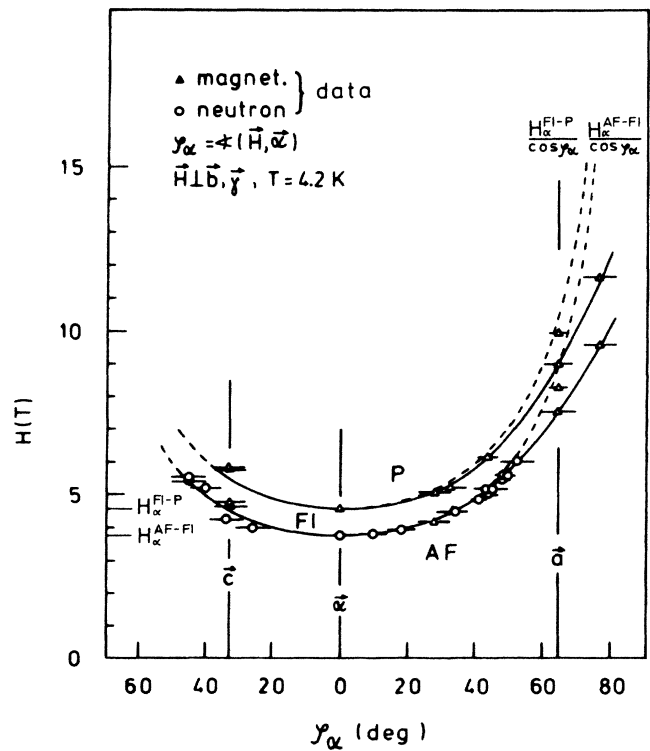


FIG. 5. Transition fields  $H^{\text{AF-FI}}$  and  $H^{\text{FI-P}}$  of  $\text{FeCl}_2 \cdot 2\text{H}_2\text{O}$  at 4.2 K for different applied field directions within the  $a$ - $c$  plane.

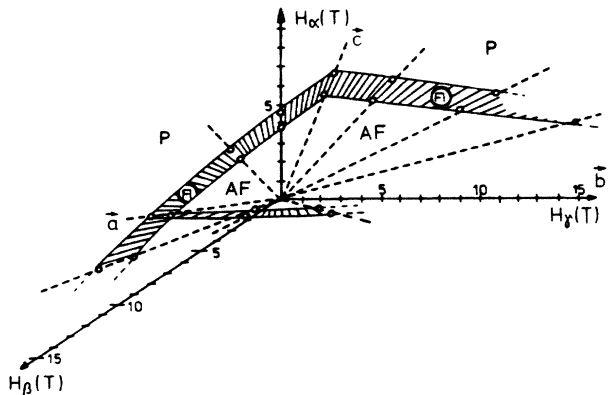


FIG. 6. Magnetic phase diagram of  $\text{FeCl}_2 \cdot 2\text{H}_2\text{O}$  at 4.2 K in the  $H_\alpha$ - $H_\beta$ - $H_\gamma$  space. Hatched planes show the measured regions of the FI phase.

term  $D=9.58 \text{ cm}^{-1}$ . The given values for the constants  $J_1, J_2,$  and  $D$  result from far-infrared experiments.<sup>8</sup> Unfortunately, in these experiments, a value for  $J_0$  could not be determined. The above value of  $J_0$  results from Raman spectroscopy experiments.<sup>9</sup>

It should be emphasized that the given values of the constants  $J_0$  and  $D$  are the subject of debate. A value of  $D=5.8 \text{ cm}^{-1}$  that actually corresponds to the value  $J_0=1.9 \text{ cm}^{-1}$  cited above is obtained as a result of calcu-

lations of the sublattice magnetization.<sup>9</sup> Independently from these studies, calculations of an  $H_\alpha$ - $T$  phase diagram yield the values  $J_0=0.58 \text{ cm}^{-1}, J_1=-0.307 \text{ cm}^{-1}, J_2=-0.032 \text{ cm}^{-1}, J_3=0.007 \text{ cm}^{-1},$  and  $D=9.5 \text{ cm}^{-1}$ .<sup>10</sup> In fact, two very different pairs of values for  $J_0$  and  $D$  exist:  $J_0=1.9 \text{ cm}^{-1}$  and  $D=5.8 \text{ cm}^{-1}$  on one side<sup>9</sup> and  $J_0=0.58 \text{ cm}^{-1}$  and  $D=9.5 \text{ cm}^{-1}$  on the other side.<sup>10</sup> With regard to this contradiction, a third estimate with  $J_0=1.0 \text{ cm}^{-1}$  was carried out, to which the calculations of the sublattice magnetization give the value  $D=9.58 \text{ cm}^{-1}$ .<sup>9,11</sup> In two cases,<sup>8,12</sup> the isotropic exchange constants  $J_0, J_1,$  and  $J_2$  are replaced by anisotropic ones; however, there exists no agreement about the kind and degree of anisotropy. We find that such additional anisotropic exchange constants do not improve the agreement between experimental and theoretical phase diagrams substantially.

Given this situation, new experiments can be helpful. For instance, the behavior of the system in magnetic fields out of the easy direction  $\alpha$  has not been studied experimentally apart from the low-field susceptibility experiments mentioned above.<sup>1</sup> The aim of our work is just

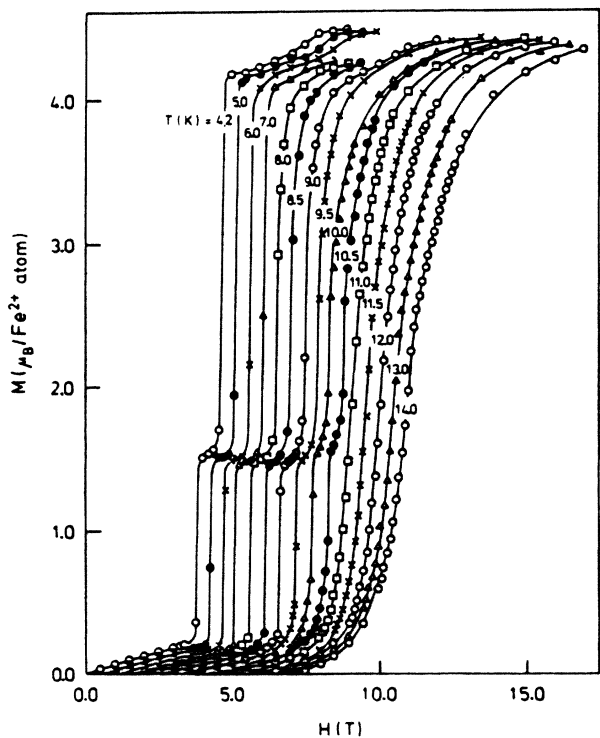


FIG. 7. Temperature dependence of magnetization measurements of  $\text{FeCl}_2 \cdot 2\text{H}_2\text{O}$  along the easy direction  $\alpha$ .

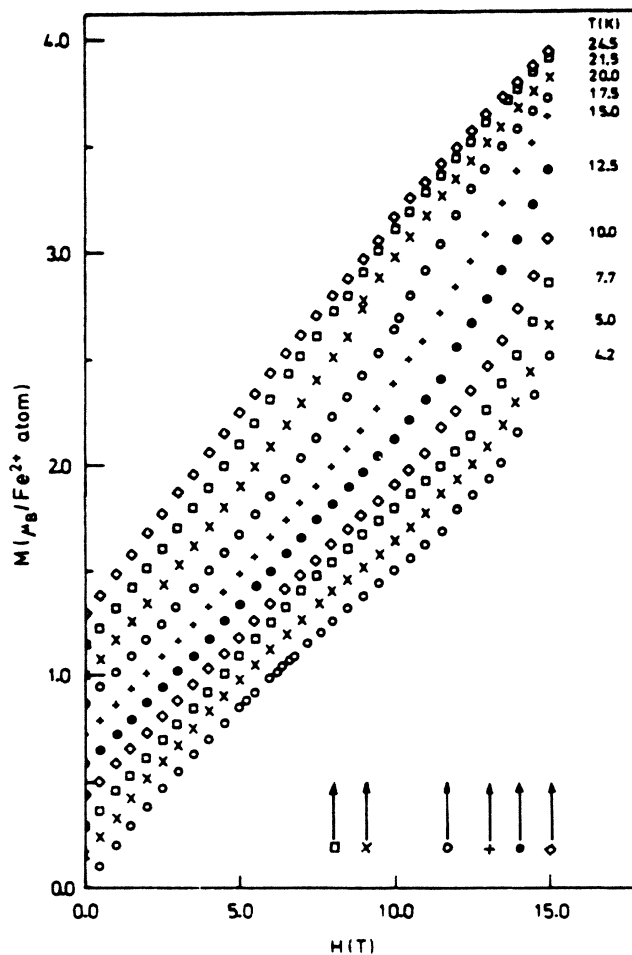


FIG. 8. Magnetization measurements of  $\text{FeCl}_2 \cdot 2\text{H}_2\text{O}$  along the intermediate direction  $\beta$  in dependence of the temperature.

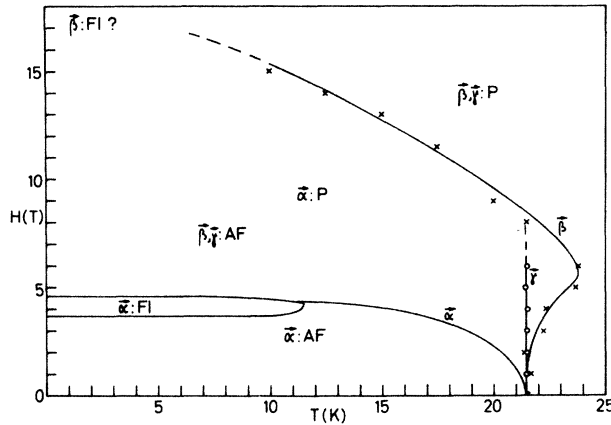


FIG. 9. Magnetic phase diagrams of  $\text{FeCl}_2 \cdot 2\text{H}_2\text{O}$  for applied fields along the principal axes  $\alpha$ ,  $\beta$ , and  $\gamma$ .

such an examination. This will enable us to demonstrate the possibility of getting substantially new results about the magnetism of the system. In Sec. II our experiments are described; in Sec. III calculations of magnetic phase diagrams of FC2 follow and are compared with the experimental results. In Sec. IV these results are compared and discussed with analogous experiments on the similar system  $\text{CoCl}_2 \cdot 2\text{H}_2\text{O}$  (CC2) and other systems.

## II. EXPERIMENTS

Neutron diffraction experiments were performed using the two-circle diffractometer, P49, of our institute at the research reactor FR2, Karlsruhe.<sup>13</sup> For these experiments, a large-gap superconducting split-pair  $\text{Nb}_3\text{Sn}$  magnet with fields up to 6.4 T was used. The geometry of this double-coil magnet enables us to perform experiments with various field directions lying within the diffraction plane in addition to experiments with the field

direction vertical to the diffraction plane. AF and FI reflections appear and disappear at different reciprocal-lattice points, and hence by these measurements it is very easy to identify the various magnetic phases belonging to the observed transition fields. Magnetization experiments alone cannot definitely determine the kind of ordered phases belonging to the observed jumps or the anomalous changes in the slopes of the magnetization curves. The antiferromagnetic and ferrimagnetic phases, observed in the neutron diffraction experiments, are identical to our former studies as described in the Introduction<sup>2,3</sup> and will be discussed no further. By means of magnetization experiments which we carried out at the high-field-magnet laboratory of the Max-Planck Institut für Festkörperforschung at the Centre National de Recherche Scientifique (CNRS) in Grenoble, France, it was possible to extend the limit of the applied field up to 15 T.

Figures 2, 3, and 4 show the magnetization curves at 4.2 K. Figure 5 summarizes the transition fields of the  $a$ - $c$  plane measured by neutron diffraction and magnetization experiments. Figure 6 gives an  $H_\alpha$ - $H_\beta$ - $H_\gamma$  phase diagram at 4.2 K in which the regions are hatched where the FI phase is observed. Magnetization curves at different temperatures and with fixed directions  $H_\alpha$  and  $H_\beta$  are shown in Figs. 7 and 8. It should be pointed out that no phase transition seems to be observed at 4.2 K up to 15 T on the  $\beta$  axis according to Figs. 2 and 8. However, Fig. 8 yields the additional information that this phase transition takes place at or perhaps slightly above 15 T. In measurements with fields along the  $\gamma$  axis which were carried out between 4.2 and 21.5 K (not shown in the figures), such swings in the magnetization curves have not been found. Therefore, there is no indication of a phase transition for fields along the direction  $\gamma$  up to 15 T. Figure 9 shows the  $H_\beta$ - $T$  phase diagram from neutron diffraction up to 6.4 T and from magnetization experiments between 8 and 15 T (arrows in Fig. 8). The  $H_\gamma$ - $T$  phase diagram, as far as was accessible with the neutron diffraction experiment, is also shown in Fig. 9. The  $H_\alpha$ - $T$  phase diagram in Fig. 9 is taken from our old experi-

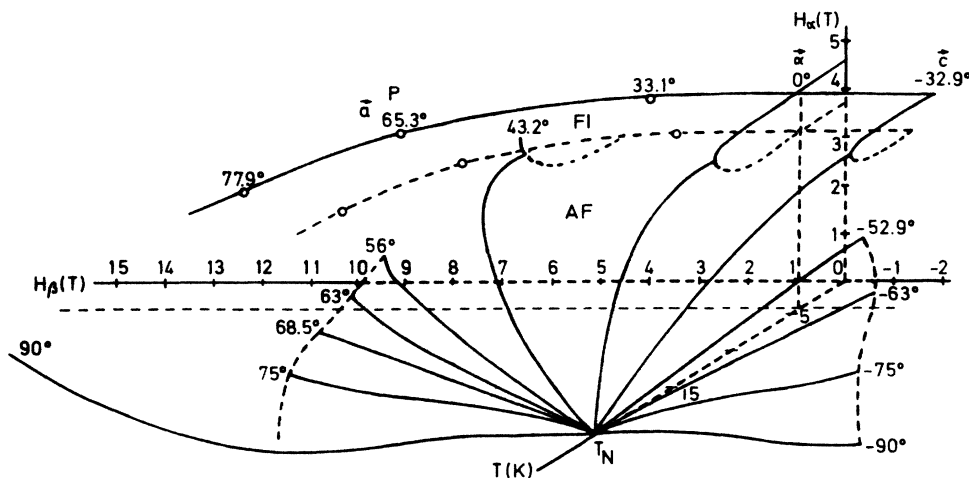


FIG. 10. Magnetic  $H_\alpha$ - $H_\beta$ - $T$  phase diagram of  $\text{FeCl}_2 \cdot 2\text{H}_2\text{O}$ .

ments.<sup>4</sup> Figure 10 summarizes the temperature-dependent experiments in an  $H_\alpha$ - $H_\beta$ - $T$  phase diagram. This last figure, in particular, suggests that the FI phase exists on the  $\beta$  axis.

### III. CALCULATIONS OF $H_\alpha$ - $H_\beta$ PHASE DIAGRAMS

The aim of our calculations is to examine the validity of the values of the constants given above by comparing

$$-F_{AF} = 2S^2 \left[ \frac{1}{2}(J_0 - |J_2|) (\cos^2\phi_1 + \cos^2\phi_2 + \cos^2\theta_1 + \cos^2\theta_2 + \cos^2\psi_1 + \cos^2\psi_2) \right. \\ \left. - 2|J_1| (\cos\phi_1\cos\phi_2 - \cos\theta_1\cos\theta_2 - \cos\psi_1\cos\psi_2) \right] + \frac{1}{2}g^{BB}\mu_B SH_\beta (\cos\phi_1 + \cos\phi_2) \\ + \frac{1}{2}g^{AA}\mu_B SH_\alpha (\cos\theta_1 - \cos\theta_2) + D \left( \frac{1}{2}S^2\cos^2\theta_1 + \frac{1}{2}S^2\cos^2\theta_2 - \frac{1}{3}S^2 - \frac{1}{3}S \right)$$

and

$$-F_{FI} = \frac{S^2}{6} \left[ (8J_0 - 8|J_1| - 4|J_2|) (\cos^2\theta_1 + \cos^2\phi_1 + \cos^2\psi_1) + 4J_0 (\cos^2\theta_2 + \cos^2\phi_2 + \cos^2\psi_2) \right. \\ \left. + (16|J_1| + 8|J_2|) (\cos\theta_1\cos\theta_2 - \cos\phi_1\cos\phi_2 - \cos\psi_1\cos\psi_2) \right] \\ + \frac{1}{3}g^{BB}\mu_B SH_\beta (2\cos\phi_1 + \cos\phi_2) + \frac{1}{3}g^{AA}\mu_B SH_\alpha (2\cos\theta_1 - \cos\theta_2) + D \left( \frac{2}{3}S^2\cos^2\theta_1 + \frac{1}{3}S^2\cos^2\theta_2 - \frac{1}{3}S^2 - \frac{1}{3}S \right).$$

Here,  $S=S_1=S_2=2$  represents the spin;  $\mu_B$ , the Bohr magneton; and  $H_\alpha$  and  $H_\beta$  are the  $\alpha$  and  $\beta$  components of the applied magnetic field. The  $\gamma$  component  $H_\gamma$  of the field is omitted in the equations. The  $g$  factors amount to  $g^{AA}=2.23$  and  $g^{BB}=2.1$ .<sup>8</sup> The values of  $J_0$ ,  $J_1$ ,  $J_2$ , and  $D$  have already been given in the Introduction. The angles  $\theta_1$ ,  $\theta_2$ ,  $\phi_1$ ,  $\phi_2$ ,  $\psi_1$ , and  $\psi_2$  are the angles of the spin vectors  $\mathbf{S}_1$  and  $\mathbf{S}_2$  with respect to the  $\alpha$ ,  $\beta$ , and  $\gamma$  axes and are defined in Fig. 11. The calculation of these angles for fixed constants as a function of the applied field can be made directly by means of calculations of partial differentials and minimalization of the free energies  $F_{AF}$  and  $F_{FI}$ , respectively. However, it is easier to find these angles by their systematic variation. Equating the

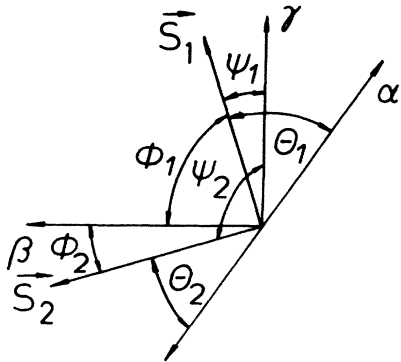


FIG. 11. Position of the spin vectors  $\mathbf{S}_1$  and  $\mathbf{S}_2$  relative to the directions  $\alpha$ ,  $\beta$ , and  $\gamma$  of the principal axes.

experimental and theoretical  $H_\alpha$ - $H_\beta$  phase diagrams and, in particular, to clarify the contradiction among the published values of the single-ion anisotropy  $D$ .

From our neutron diffraction experiments, it is known that only the two-sublattice AF and FI phases and the  $P$  phase exist.<sup>2,3</sup> Therefore, the free energy  $F$  can be calculated as a function of two spin vectors  $\mathbf{S}_1$  and  $\mathbf{S}_2$  in all three phases. At 0 K the following is valid:

minimal free energies of the three phases AF, FI, and  $P$  by pairs, we finally get the phase boundaries between the phases. Such calculations were performed on the IBM 3090-200 computer of the Technische Hochschule Darmstadt. For  $H_\gamma=0$  and for the evaluated values of the constants, both spin vectors remain in the  $\alpha$ - $\beta$  plane. Therefore, with  $\psi_1=\psi_2=90^\circ$ ,  $\phi_1=90^\circ\pm\theta_1$ , and  $\phi_2=\pm(90^\circ-\theta_2)$  simple formulas for the transition fields can be calculated, especially for the two cases  $\mathbf{H}=(H_\alpha,0,0)$  and  $\mathbf{H}=(0,H_\beta,0)$ . For the transitions on the  $\alpha$  axis, the already known transition fields are obtained:<sup>14</sup>

$$H_\alpha^{AF-FI} = \frac{S}{g^{AA}\mu_B} (8|J_1| - 8|J_2|),$$

$$H_\alpha^{AF-P} = \frac{S}{g^{AA}\mu_B} |J_1| \quad (\text{not realized in FC2}),$$

$$H_\alpha^{FI-P} = \frac{S}{g^{AA}\mu_B} (8|J_1| + 4|J_2|).$$

The constants  $J_1$  and  $J_2$  can be calculated directly from the observed transition fields  $H_\alpha^{AF-FI}$  and  $H_\alpha^{FI-P}$ . Therefore, these two constants are known very well in contrast to the values of  $J_0$  and  $D$ .

A spin-flop phase does not exist on the  $\alpha$  axis. Therefore, a lower limit for the single-ion anisotropy can be estimated. For the transition field from a spin-flop phase with the same unit cell as the AF phase to the saturated paramagnetic phase, we find

$$H_\alpha^{SF-P} = \frac{2S}{g^{AA}\mu_B} (8|J_1| - D).$$

If the spin-flop phase exists, it appears in the phase diagram at the field  $H_\alpha^{\text{FI-P}}$  for the smallest possible value of  $D$ . Because it was not observed, it must be valid that  $H_\alpha^{\text{SF-P}} < H_\alpha^{\text{FI-P}}$  and therefore

$$D > 4|J_1| - 2|J_2| = 0.99 \text{ cm}^{-1}.$$

For the AF-P transition on the  $\beta$  axis, we find

$$H_\beta^{\text{AF-P}} = \frac{2S}{g^{\beta\beta}\mu_B} (8|J_1| + D)$$

and for the FI-P transition approximately

$$H_\beta^{\text{FI-P}} \approx \frac{2S}{g^{\beta\beta}\mu_B} (6|J_1| + 3|J_2| + D).$$

As shown in Sec. II, it is not clear which of these two transitions exists in FC2. In this situation, it is worthwhile to summarize the last two equations

$$H_\beta^{\text{FI-P}} \approx H_\beta^{\text{AF-P}} - \frac{2S}{g^{\beta\beta}\mu_B} (2|J_1| - 3|J_2|).$$

Using the values for the constants mentioned above we get

$$H_\beta^{\text{FI-P}} \approx H_\beta^{\text{AF-P}} - 1.66 \text{ T}.$$

If one calculates the transition field  $H_\beta^{\text{AF-P}}$  using the given values of the constants, one finds  $H_\beta^{\text{AF-P}} = 47.9 \text{ T}$ , a value about three times as high as expected from Figs. 8–10. Obviously, the value for the single-ion anisotropy  $D$  in the formula for  $H_\beta^{\text{AF-P}}$  is responsible for this discrepancy because its value is known with the least certainty. Indeed, a value  $D = 1.52 \text{ cm}^{-1}$  yields the phase transition at the observed place. However, the problem is not only that this value deviates considerably from both the published values  $D = 9.58 \text{ cm}^{-1}$  and  $D = 5.8 \text{ cm}^{-1}$ , but also that a calculated  $H_\alpha$ - $H_\beta$  phase diagram with  $D = 1.52 \text{ cm}^{-1}$  contradicts our observed phase diagram with respect to the phase boundaries within the  $H_\alpha$ - $H_\beta$  plane. It includes a triple point at  $H_\alpha^T = 3.9 \text{ T}$  and  $H_\beta^T = 6.8 \text{ T}$  which we cannot detect over the entire measured region of the phase diagram. Therefore, a simple changing of the value of  $D$  cannot help to obtain better agreement between experiments and calculations. Figure 12(a) shows as an example a calculated phase diagram for this model with isotropic exchange constants. It is calculated with the values  $J_0 = 1.90 \text{ cm}^{-1}$ ,  $J_1 = -0.28 \text{ cm}^{-1}$ ,  $J_2 = -0.039 \text{ cm}^{-1}$ , and  $D = 1.44 \text{ cm}^{-1}$ . These values of  $J_1$  and  $J_2$  result from our own experimental values of the transition fields  $H_\alpha^{\text{AF-FI}} = 3.70 \text{ T}$  and  $H_\alpha^{\text{FI-P}} = 4.60 \text{ T}$ .<sup>4</sup> They are modified only slightly relative to the above-mentioned values  $J_1 = -0.27 \text{ cm}^{-1}$  and  $J_2 = -0.044 \text{ cm}^{-1}$ , which belong to transition fields  $H_\alpha^{\text{AF-FI}} = 3.50 \text{ T}$  and  $H_\alpha^{\text{FI-P}} = 4.50 \text{ T}$ .<sup>8</sup> The value  $D = 1.44 \text{ cm}^{-1}$  is taken in order to get  $H_\beta^{\text{AF-P}} = 15 \text{ T}$ .

This situation demands that the anisotropy of the system be represented not only by one constant  $D$  but by anisotropic exchange constants  $J_0$ ,  $J_1$ , and  $J_2$ . For this case, it is not necessary to consider the constant  $D$  separately in the formulas for the  $H_\alpha$ - $H_\beta$  plane. Rather, one can sum the component  $J_0^\alpha$  of  $J_0$  and  $D$  to a new component

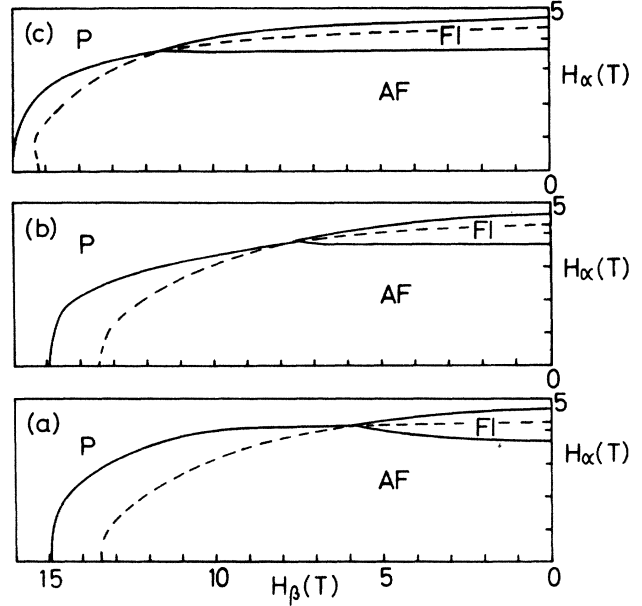


FIG. 12. (a)–(c) Calculated magnetic phase diagram of  $\text{FeCl}_2 \cdot 2\text{H}_2\text{O}$  for the  $H_\alpha$ - $H_\beta$  plane at 0 K. (a) Isotropic exchange constants; (b) anisotropic exchange constants; (c) isotropic exchange constants and field-dependent single-ion anisotropy.

$J_0^\alpha = J_0^\alpha + D/2$ . Doing so introduces only two additional constants  $J_1^\beta$  and  $J_2^\beta$  in this model; the  $\gamma$  components are irrelevant, if we restrict the calculations to the  $H_\alpha$ - $H_\beta$  plane. The new equations for the free energies are omitted here. Now, one can vary the values of the constants again. Figure 12(b) gives one example with the values  $J_0^\alpha = 2.92 \text{ cm}^{-1}$ ,  $J_0^\beta = 1.90 \text{ cm}^{-1}$ ,  $J_1^\alpha = -0.28 \text{ cm}^{-1}$ ,  $J_1^\beta = -0.14 \text{ cm}^{-1}$ ,  $J_2^\alpha = -0.039 \text{ cm}^{-1}$ , and  $J_2^\beta = -0.0195 \text{ cm}^{-1}$ . Even though we suppose considerable anisotropies, the phase diagram is not qualitatively changed.

In the anisotropic model we evaluate

$$H_\beta^{\text{AF-P}} = \frac{4S}{g^{\beta\beta}\mu_B} (J_0^\alpha - J_0^\beta + 2|J_1^\alpha| + 2|J_1^\beta| - |J_2^\alpha| + |J_2^\beta|)$$

and approximate

$$H_\beta^{\text{FI-P}} \approx \frac{2S}{g^{\beta\beta}\mu_B} (2J_0^\alpha - 2J_0^\beta + 2|J_1^\alpha| + 4|J_1^\beta| + |J_2^\alpha| + 2|J_2^\beta|);$$

this implies

$$H_\beta^{\text{FI-P}} \approx H_\beta^{\text{AF-P}} - \frac{2S}{g^{\alpha\alpha}\mu_B} (2|J_1^\alpha| - 3|J_2^\alpha|).$$

The formulas for the three transition fields on the  $\alpha$  axis are identical to those of the isotropic model, if one replaces  $J_1$  and  $J_2$  by  $J_1^\alpha$  and  $J_2^\alpha$ . That means that the constants  $J_1^\alpha$  and  $J_2^\alpha$  are known from the observed values of

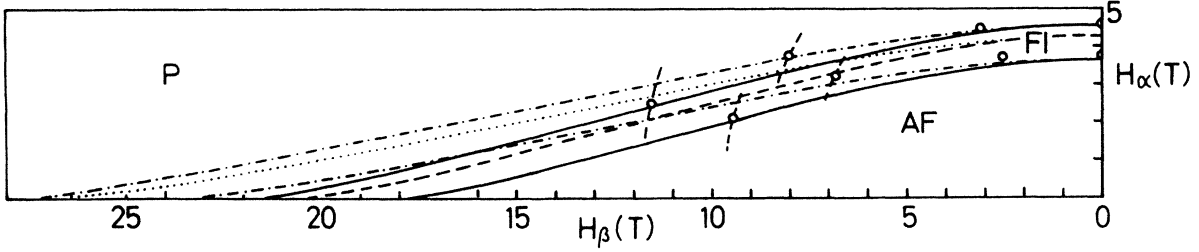


FIG. 13. Experimental phase diagram of  $\text{FeCl}_2 \cdot 2\text{H}_2\text{O}$  for the  $H_\alpha$ - $H_\beta$  plane at 4.2 K and two calculated phase diagrams at 0 K (see text for explanations).

$H_\alpha^{\text{AF-FI}}$  and  $H_\alpha^{\text{FI-P}}$ . Therefore, the difference  $H_\beta^{\text{AF-P}} - H_\beta^{\text{FI-P}}$  is also known; it amounts to 1.70 T. Particularly, Fig. 10 suggests that the FI phase exists on the  $\beta$  axis. Therefore, instead of the equation  $H_\beta^{\text{AF-P}} - H_\beta^{\text{FI-P}} \approx 1.70$  T, the relation  $H_\beta^{\text{FI-P}} > H_\beta^{\text{AF-P}}$  follows.

This last relation implies  $|J_2^\alpha| > \frac{2}{3}|J_1^\alpha|$ , a condition which is absolutely not fulfilled by the known values  $|J_1^\alpha| = 0.28 \text{ cm}^{-1}$  and  $|J_2^\alpha| = 0.039 \text{ cm}^{-1}$ . Under these circumstances, the anisotropic model must also be rejected. In principle, the possibility exists to extend the number of constants further by introducing off-diagonal elements of exchange and  $g$  tensors or by adding further exchange constants  $J_3$ , etc. Increasing the number of constants in this way seems to be inadequate due to the limitations of the presently known experimental data.

One can return to the isotropic model and try to understand the experiments by introducing the field-dependent constants  $\bar{D}$ ,  $\bar{J}_0$ ,  $\bar{J}_1$ , and  $\bar{J}_2$ . Simple phenomenological linear terms in the field with three constants  $k_1$ ,  $k_2$ , and  $k_3$  yield

$$|\bar{J}_1| = |J_1^0| (1 - k_1 H),$$

$$|\bar{J}_2| = |J_2^0| (1 - k_2 H),$$

$$\bar{D} = D^0 (1 - k_3 H),$$

and for the transition fields

$$H_\alpha^{\text{AF-FI}} = \frac{8S |J_1^0| - 8S |J_2^0|}{g^{\alpha\alpha} \mu_B + 8S |J_1^0| k_1 + 8S |J_2^0| k_2},$$

$$H_\alpha^{\text{AF-P}} = \frac{8S |J_1^0|}{g^{\alpha\alpha} \mu_B + 8S |J_1^0| k_1} \quad (\text{not realized in FC2}),$$

$$H_\alpha^{\text{FI-P}} = \frac{8S |J_1^0| + 4S |J_2^0|}{g^{\alpha\alpha} \mu_B + 8S |J_1^0| k_1 - 4S |J_2^0| k_2},$$

$$H_\beta^{\text{AF-P}} = \frac{16S |J_1^0| + 2D^0 S}{g^{\beta\beta} \mu_B + 16S |J_1^0| k_1 + 2D^0 S k_3},$$

$$H_\beta^{\text{FI-P}} \approx \frac{12S |J_1^0| + 6S |J_2^0| + 2D^0 S}{g^{\beta\beta} \mu_B + 12S |J_1^0| k_1 - 6S |J_2^0| k_2 + 2D^0 S k_3}.$$

By coupling the formulas of the isotropic model with these new formulas, one finds the relations

$$J_2^0/J_1^0 = J_2/J_1, \quad k_1 = \frac{g^{\alpha\alpha} \mu_B}{8S} \left( \frac{1}{J_1} - \frac{1}{J_1^0} \right), \quad \text{and } k_2 = 0.$$

Similar formulas for  $D^0$  and  $k_3$  dependent on the old constants are too complicated to give here; nevertheless, they are easily found by elementary arithmetic. From the relation  $k_2 = 0$  the linear dependence

$$2H_\alpha^{\text{FI-P}} + H_\alpha^{\text{AF-FI}} = 3H_\alpha^{\text{AF-P}}$$

follows; consequently, one cannot evaluate the five formulas for the transition fields in order to determine  $J_1^0$ ,  $J_2^0$ ,  $D^0$ ,  $k_1$ , and  $k_3$ . Rather, it is necessary to fit the phase diagram by trial and error methods. Starting with the known values of  $S$ ,  $g^{\alpha\alpha}$ ,  $g^{\beta\beta}$ ,  $J_1$ , and  $J_2$ , the value of  $k_1$  was varied systematically.

Two kinds of phase diagrams appear. We can discuss them by means of the two special cases  $k_1 = k_2 = 0$ ,  $k_3 \neq 0$  and  $k_1 \neq 0$ ,  $k_2 = k_3 = 0$ . In the first case, the field dependence exists only for the single-ion anisotropy; one gets phase diagrams of the former kind as one with  $k_3 = 0.04659 \text{ T}^{-1}$ ,  $J_1^0 = -0.28 \text{ cm}^{-1}$ ,  $J_2^0 = -0.039 \text{ cm}^{-1}$ , and  $D^0 = 6.611 \text{ cm}^{-1}$  is shown in Fig. 12(c). Such diagrams contain a triple point and do not improve the correspondence. Figure 13 shows two diagrams for the second case with  $k_1 \neq 0$  and  $k_2 = k_3 = 0$ . Only the exchange constant  $\bar{J}_1$  depends on the field. Particularly, the FI phase now exists on the  $\beta$  axis. The chosen parameters are  $k_1 = 0.04848 \text{ T}^{-1}$ ,  $J_1^0 = -0.354 \text{ cm}^{-1}$ ,  $J_2^0 = -0.0493 \text{ cm}^{-1}$ , and  $D^0 = 5.734 \text{ cm}^{-1}$  for the phase diagram with solid lines and  $k_1 = 0.03638 \text{ T}^{-1}$ ,  $J_1^0 = -0.332 \text{ cm}^{-1}$ ,  $J_2^0 = -0.0463 \text{ cm}^{-1}$ , and  $D^0 = 6.229 \text{ cm}^{-1}$  for the diagram with dashed-dotted lines. The experimental accuracy was determined by the accuracy with which the crystals could be oriented against the field direction. In light of this latter inaccuracy, the observed and calculated diagrams are in agreement.

#### IV. DISCUSSION

The possibility exists to improve the agreement between observed and calculated diagrams by using more computer time. This is of limited value as long as our phenomenological model cannot be replaced by a physical one. The most obvious starting point is the fact that

the spin system does not exist in the ground state due to the influence of high Zeeman terms, as in our case. But the ground state and excited states are mixed and this destroys the assumption of field-independent system constants. Surprisingly, the introduction of only one field-dependent exchange constant was sufficient to yield agreement between experiment and calculation.

The compound CC2 has magnetic properties very similar to the system FC2.<sup>15,16</sup> But in CC2, the easy direction is along the  $b$  axis, and the exchange constants  $J_0$ ,  $J_1$ , and  $J_2$  are anisotropic in any case. For that, a single-ion anisotropy  $D$  does not exist in CC2. For the principal axes of the susceptibility tensor, magnetization experiments were performed up to 40 T and at 1.3 K.<sup>17</sup> They are absent along other directions. Further, it has not been proved by neutron diffraction or any other method what kind of magnetic phases exist in applied fields apart from the easy direction. In summary, the only useful result concerning our present discussion is a change of the slope in the magnetization curve for the intermediate axis at 16.2 T which is interpreted as a phase transition from the AF to the  $P$  phase.<sup>17</sup> A value of 24 T is calculated for this transition field. From that point of view, the problem is similar to that of FC2. But, if one takes into account the one (and only one) bend in the magnetization curve, a triple point must exist in CC2 in the plane between the easy and the intermediate directions. The authors<sup>17</sup> do not explain the reduction of the transition field by changing the values of the constants, though no experiments within this plane forbid this. They retain the well-known values of all constants used. As we have done for FC2, they introduce nonlinear terms to the field in the free energies.

Temperature-dependent phase diagrams have been calculated for FC2 only for the case of  $H_\alpha$ - $T$  diagrams<sup>18,10</sup> and have been compared with experimental diagrams.<sup>10,4</sup> For other field directions, they do not exist, so that we must depend upon comparisons with other compounds. Our essential result, shown in Fig. 9, is the increasing AF- $P$  transition temperature for the field direction along the  $\beta$  axis. The ascent amounts to 2.5 K. For fields along the  $\gamma$  axis, we can detect neither an increase nor decrease of the phase boundary up to 6 T, nor the beginning of a phase transition in the constant-temperature magnetization curves up to 15 T. These findings are the reason the direction  $\beta$  is denoted as the intermediate direction and  $\gamma$  as the hard one. Up to now from the susceptibility data,<sup>1</sup> it was customary to denote the direction  $\alpha$  as the easy one and, neglecting a transverse anisotropy, not to differentiate between the  $\beta$  and the  $\gamma$  axes.<sup>8</sup>

The dependence in CC2 from applied fields out of the easy direction on the Néel temperature was examined by means of neutron diffraction.<sup>19</sup> Unfortunately, these experiments were restricted to special directions which were perpendicular to the easy direction but not along the two other principal axes. The restriction resulted from the geometry of our magnet together with conditions from the diffraction geometry. These two directions form angles of 24.0° and 62.7° with respect to the

hard direction of CC2. They do not show a well-pronounced increase in the Néel temperature up to 6.4 T. For CC2, but not for FC2, we observed a quasi-one-dimensional character in the critical behavior at the Néel point.<sup>4</sup> Theories give increasing phase boundaries more easily for isotropic than for anisotropic systems and more easily for lower-dimensional than for three-dimensional systems.<sup>20</sup> The ratio between interchain and intrachain interactions and, therefore, the dimensionality are nearly the same in FC2 and CC2. Therefore, the degree of anisotropy and not the dimensionality must be responsible for the different increases of the AF- $P$  phase boundaries.

In pure three-dimensional systems, increasing Néel temperatures are only known for some compounds; if they occur, it is only for the easy direction and more likely for Heisenberg systems than for Ising systems.<sup>21</sup> Examples are  $\text{RbMnF}_3$  and  $\text{CsMnF}_3$ , in which the increase amounts only 0.2 K in  $\text{RbMnF}_3$  and 0.04 K in  $\text{CsMnF}_3$ .<sup>22</sup> Larger effects are to be found in quasi-one-dimensional systems with antiferromagnetic chains, especially in  $S = \frac{5}{2}$  Heisenberg systems with small orthorhombic anisotropy.<sup>23</sup> Such systems, like  $\text{CsMnBr}_3 \cdot 2\text{H}_2\text{O}$ ,  $\text{CsMnCl}_3 \cdot 2\text{H}_2\text{O}$ , and  $(\text{CH}_3)\text{NH}_2\text{MnCl}_3$ , have spin-flop phases for applied fields along the easy direction because of their small anisotropy and in contradiction to FC2. For the intermediate and the hard directions, the results are very similar to FC2. For instance, the intermediate direction yields the largest increase of the Néel temperature while the increase for the hard direction is only moderate. For the intermediate direction of these Mn systems, values for  $T_N(H)/T_N(0)$  between 1.3 and 1.6 were found.<sup>23</sup> For FC2, this value amounts to 1.1. In the Mn compounds, the ratio of interchain to intrachain interactions varies between  $10^{-3}$  and  $7 \times 10^{-2}$ ; for FC2 one finds about 0.1–0.3. Hence, the quasi-one-dimensional character of FC2 is very small, whereas it is more pronounced in the Mn compounds. In the Mn compounds, antiferromagnetic chains are coupled antiferromagnetically, whereas in FC2, ferromagnetic chains are coupled antiferromagnetically. In general, one expects less pronounced anomalies for systems with ferromagnetic chains than for systems with antiferromagnetic chains.<sup>20</sup>

#### ACKNOWLEDGMENTS

The authors would like to thank the Kernforschungszentrum Karlsruhe, Departments Kerntechnische Betriebe (KTB/RBT) and the Institut für Nukleare Festkörperphysik (INFP) for granting the use of the beam tube at the reactor FR2, Karlsruhe. Further, we thank Professor Dr. G. Landwehr for permission to perform the magnetization experiments at the High-Field-Magnet Laboratory of the Max-Planck Institut für Festkörperforschung, Stuttgart, at the Centre National de Recherche Scientifique (CNRS) in Grenoble. This work has been funded by the German Federal Minister for Research and Technology (BMFT) under Contract Nos. 03-B41 A08-5 and 03-WL1DAR-0.

- <sup>1</sup>A. Narath, *Phys. Rev.* **139**, A1221 (1965).
- <sup>2</sup>W. Schneider and H. Weitzel, *Solid State Commun.* **13**, 303 (1973).
- <sup>3</sup>W. Schneider and H. Weitzel, *Acta Crystallogr. A* **32**, (1976).
- <sup>4</sup>J. Hirte, H. Weitzel, and N. Lehner, *Phys. Rev. B* **30**, 6707 (1984).
- <sup>5</sup>K. Inomata and T. Oguchi, *J. Phys. Soc. Jpn.* **23**, 765 (1967).
- <sup>6</sup>K. Inomata and T. Oguchi, *J. Phys. Soc. Jpn.* **28**, 905 (1970).
- <sup>7</sup>T. Oguchi, *J. Phys. Soc. Jpn.* **20**, 2236 (1965).
- <sup>8</sup>K. A. Hay and J. B. Torrance, *Phys. Rev. B* **2**, 746 (1970).
- <sup>9</sup>L. Graf, Ph.D. thesis, Technische Hochschule Darmstadt, 1977.
- <sup>10</sup>M. A. Lowe, C. R. Abeledo, and A. A. Missetich, in *Magnetism and Magnetic Materials-1971 Proceedings on the 17th Annual Conference on Magnetism and Magnetic Materials*, Chicago, AIP Conf. Proc. No. 5, edited by D. C. Graham and J. J. Rhyne (AIP, New York, 1972), pp. 307-310.
- <sup>11</sup>L. Graf, *Phys. Status Solidi B* **88**, 429 (1978).
- <sup>12</sup>L. Graf, *Z. Phys. B* **2**, 27 (1978).
- <sup>13</sup>J. Hirte and H. Weitzel, Kernforschungszentrum Karlsruhe Report No. 3381, edited by G. Heger and H. Weitzel (Kernforschungszentrum, Karlsruhe, 1982), pp. 118-122.
- <sup>14</sup>A. Narath, *Phys. Lett.* **13**, 12 (1964).
- <sup>15</sup>A. Narath, *Phys. Rev.* **136**, A766 (1964).
- <sup>16</sup>A. Narath, *Phys. Rev.* **140**, A552 (1965).
- <sup>17</sup>H. Mollmoto, M. Motokawa, and M. Date, *J. Phys. Soc. Jpn.* **49**, 108 (1980).
- <sup>18</sup>K. Yamada and J. Kanamori, *Progr. Theor. Phys.* **38**, 541 (1967).
- <sup>19</sup>J. Hirte and H. Weitzel, Kernforschungszentrum Karlsruhe Report No. 3381, edited by G. Heger and H. Weitzel (Kernforschungszentrum Karlsruhe, 1982), pp. 122 and 123.
- <sup>20</sup>T. Oguchi and M. Blume, *J. Phys. Soc. Jpn.* **50**, 2547 (1981).
- <sup>21</sup>J. M. Kosterlitz, D. R. Nelson, and M. E. Fisher, *Phys. Rev. B* **13**, 412 (1976).
- <sup>22</sup>N. F. Oliveira and Y. Shapira, *J. Appl. Phys.* **50**, 1790 (1979).
- <sup>23</sup>J. P. A. Hijmans, K. Kopinga, F. Boersma, and W. J. M. de Jonge, *Phys. Rev. Lett.* **40**, 1108 (1978).